Results of ISO/TS 6336-22 Evaluating Full Contact Zone

Robin Olson, David Talbot, Mark Michaud, Jonathan Keller, and John Amendola, Sr.

ISO/TS 6336-22 (Calculation of load capacity of spur and helical gears—Part 22: Calculation of micropitting load capacity) is the ISO technical specification containing a proposal for a calculation of risk of micropitting in gear sets (Ref. 1). ISO/TS 6336-22 calculates a safety factor against micropitting by comparing the minimum specific lubricant film thickness to the permissible lubricant film thickness. Unfortunately, ISO/TS 6336-22 does not recommend a minimum safety factor. Rather, it is left to the engineer to compare the calculated results to a similar gear application.

The approach has been published since 2010 and the "technical specification" designation of the document means that it contains calculations that are still subject to further development. The next systematic review of the document will require that it either be converted to an international standard or withdrawn. For this reason, it is important to verify that the calculations in ISO/TS 6336-22 reliably predict the risk of micropitting.

As is typical of gear calculation standards, two different methods are presented in ISO/TS 6336-22. The first, Method A, allows the engineer to calculate lubricant film thicknesses using a gear computing program that models the complete contact area of the mesh. In contrast, Method B starts with the assumption that micropitting will start in the region of negative sliding and evaluates the film thickness at specific points along the line of action. ISO/TS 6336-22 recommends both methods should be validated against experience with gear sets in similar application conditions for the calculation of the permissible specific film thickness.

A previous paper, "Case Study of ISO/TS 6336-22 Micropitting Calculation" (Ref. 2), evaluates three cases using the Method B calculations. The first example is an increasing gear set for a compressor, the second is a wind turbine gear set, and the last is the American Gear Manufacturers Association (AGMA) Tribology Test gear set. These examples cover a range of gearing sizes and application conditions. All the gear sets experienced micropitting, providing good examples to verify the computation results. Using Method B, only the AGMA Tribology Test gearing resulted in safety factors that aligned with expectations predicting micropitting.

The results for all three cases were reviewed with members of ISO Working Group 6, who were central to the development of ISO/TS 6336-22. They expressed concern about the use of Method B for Cases 1 and 2. With a pitch line velocity above 80 m/s, Case 1 requires the use of Method A according to the scope of ISO/TS 6336-22. For Case 2, ISO/IEC 61400-4 for wind turbines requires the use of Method A to calculate the minimum specific film thickness. The operating sump temperature for this drive was also scrutinized as wind turbine gearing can run at higher temperatures.

Consequently, the operating conditions and calculation parameters for all three cases were investigated further. That information has been modified for this paper. The results from the previous paper have been updated and are presented here along with the results from Method A. The results from both methods are compared in order to point out the differences. They are also compared to the field results to determine whether ISO/TS 6336-22 Method A reliably indicates micropitting will occur.

Description of ISO/TS 6336-22

The previous paper contained a detailed description of the methods in ISO/TS 6336-22. A brief refresher is presented here.

In ISO/TS 6336-22, two different methods are presented for the calculations of the minimum specific lubricant film thickness and the permissible specific film thickness. Like other ISO gear calculations, Method A involves the use of testing or detailed calculations to determine critical parameters. Method B is a simplified, analytical method for each. Method B was used in the previous paper.

It is possible to calculate the minimum specific film thickness in the numerator of the safety factor using one method and the permissible specific film thickness in the denominator of the safety factor using the opposite method.

Method B

Method B calculations were conducted using a Mathcad worksheet to follow the equations found in ISO/TS 6336-22.

Minimum specific film thickness

A calculation of the minimum specific film thickness using Method B begins by calculating the film thickness with a Dowson/Higginson analysis along the line of action. This value is modified by a local sliding factor that accounts for regions of negative sliding. The minimum of the specific film thicknesses along the line of action is used to calculate the safety factor.

Permissible specific film thickness

The permissible specific film thickness is determined by conducting standardized testing with gearing that is similar in geometry, quality, and material of the gearing being designed. The gearing is run until the micropitting failure limit is reached. The critical specific film thickness for the test gearing is then calculated with ISO/TS 6336-22 using the load data from the failure stage. This is the permissible specific film thickness. If it is not possible to test with real gears, one may use the failure load stage of the lubricant in standardized tests, such as FVA 54 (Ref. 3), and calculate the minimum specific film thickness using the test gearing.

Method A

Minimum specific film thickness

To determine the minimum specific lubricant film thickness using Method A, the engineer calculates the value with a gear computing program that models the complete contact area of the mesh. The load distribution, sliding velocities, and actual service conditions are considered in this analysis. The results appear as maps of pressures and film thicknesses across the face of the pinion and gear flanks. These are used to calculate the specific lubricant film thickness at each point in the contact zone. It is important to note that the minimum value is used for the safety factor against micropitting.

Permissible specific film thickness

The permissible specific film thickness is determined through testing of real gears in conditions like the application until micropitting just occurs. The test loads and the gear computing program are then used to calculate the film thickness. These tests can also be performed for gear designs and service conditions very similar to the gear set of interest. However, testing such as this can be very costly and may not always be practical if the applications are high load, low speed, with varying operating conditions, and low production volume, or noncritical service. If that is the case, there are options to approximate the permissible specific film thickness from reference gears and FZG lubricant tests. However, each approximation reduces the accuracy of the resulting safety factor.

As recommended in ISO/TS 6336-22, it is important to interpret the micropitting safety factor by comparing it to the performance of similar gearing used in the field under similar operating conditions.

Application of Method A in This Paper

As can be seen in the preceding clauses, a true Method A calculation of the permissible specific film thickness requires that real gearing be tested in a controlled test until micropitting occurs. In Cases 1 and 2, this was not possible given their applications, size, and load conditions. The calculations here were done using Method A for the minimum specific film thickness in the numerator and Method B for the permissible value in the denominator of the safety factor calculation.

Method A Gear Computation Program–*WindowsLDP*

There are several gear computing programs capable of calculating the Hertzian stresses in the contact zone of a gear tooth mesh. This paper uses the *WindowsLDP* (Load Distribution Program) from The Ohio State University to determine the stresses. The remainder of the factors follows the methods of ISO/TS 6336-22 to calculate the minimum specific film thickness.

WindowsLDP is a quasistatic gear design and analysis tool for external and internal spur and helical gear pairs. It employs computationally efficient and accurate semianalytical formulations to compute the load distribution between multiple mating teeth of gears.

The contact pressure distribution is calculated using a parallel-axis gear pair load distribution model (Ref. 4). This model combines:

- The unloaded tooth contact analysis proposed by Singh and Houser (Ref. 5),
- Sources of compliance including tooth bending and shear (Ref. 6),
- Tooth base rotation (Ref. 7) and contact deformation (Ref. 8),
- An initial separation vector including any deviations of the surfaces from perfect involutes (i.e., microgeometry modification).

The load distribution is computed by implementing the modified simplex algorithm proposed by Conry and Seireg (Ref. 9).

WindowsLDP has been validated against testing throughout its development.

Using the predicted load distribution, *WindowsLDP* computes the loaded transmission error, root and contact stress distributions, mesh stiffness functions, and tooth forces. Other design evaluation parameters such as lubricant film thickness and

surface temperature can also be computed. Tooth modifications of various forms can be entered interactively or can be read from the tooth surface measurements. The results are presented by an interactive graphical user interface that provides the user the flexibility to process and present them in desired formats.

Case Studies Using Method A

Cases of operating gear sets that experienced micropitting were selected to exercise the ISO/TR 6336-22 document. Because there was concern over the influence of operations and maintenance on micropitting, the authors reviewed lubrication tests, load cases, and operating conditions for each, particularly for Cases 1 and 2. The details of the calculations of these case studies are quite lengthy. The drawings and details of the profile and lead modifications are also proprietary. The authors can provide specific details upon request.

Case 1—High-Speed Compressor Gear Set

Case 1 is a high-speed gear set driving a centrifugal compressor. This set had micropitting on the pinion starting in the dedendum, extending through the pitch line and to the addendum. The micropitting is localized to the drive end of the face width. From experience, this result is predictable due to an increase in tooth contact temperature as the gear mesh load travels through the helical contact pattern.

This gearbox operated for approximately 120,000 hours or 54.6 x 109 cycles. The installation was not located near an area of salt water, high humidity, or subject to significant climatic temperature fluctuations. It operated continuously for four- to five-year periods of time under constant load and speed in an environmentally controlled room. This continuous operation prohibited the absorption of water into the lubricant. After every four to five years of operation, the gearbox was shut down, inspected, and routinely maintained. It was not until approximately 13.5 years of operation that micropitting was detected. At this point, the gear set was exchanged. Prior to this, there was no significant maintenance required.

A picture of the micropitting damage can be seen in Figure 1, with more detail in the previous paper. Other than micropitting, the rest of the gear tooth surface is in very good condition and there are no indications of contact distress or scuffing.

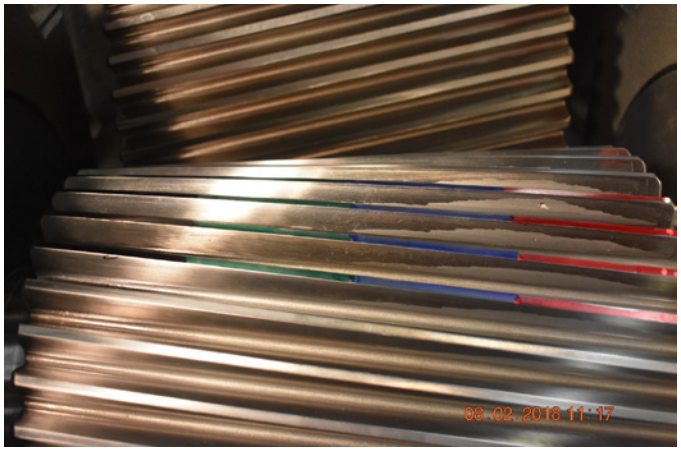

Figure 1—Micropitting on the flank of the pinion teeth. The red zone is closest to the compressor (drive end). The black zone is the motor side. (Photo courtesy of Artec Machine Systems.)

The geometry, loads, and lubricant for this case are summarized in Table 1. The gear teeth have adequate profile and lead modifications for the operating loads.

Dimension	Units	Pinion	Gear
Number of teeth	-	37	163
Ratio	-	4.405	
Center distance	mm	600	
Normal module	mm	5.90	
Face width	mm	280	
Outside diameter	mm	236.30	987.29
Pressure angle	degrees	20.00	
Helix angle	degrees	10.00	
Addendum modification coefficient	-	0.2407	-0.0876
Surface roughness	µm	0.41	0.40
ISO accuracy grade	-	4	4
Material surface hardness	HRC	58-64	58-64
Pinion speed	rpm	7,582.0	
Pinion torque	N-m	12,209.3	
$K_A K_v K_{H\alpha} K_{H\beta}$ product	-	1.4170	
Lubricant	-	Mobil Teresstic AC ISO VG 32	
Inlet lubricant temperature (estimated)	°C	54	
Bulk temperature (for calculations)	°C	82.93/100	

Table 1—Input data for Case 1.

Lubricant Condition

The lubricant used in this gear drive was Mobil Teresstic AC 32. This is an ISO VG 32 rust and oxidation oil. Light lubricants such as this are typically used in compressor-duty gear drives wherein there is a long history of successful use.

After detection of micropitting, a sample of this lubricant was analyzed compositionally using ferrography and comparing it to a sample of new lubricant. The analyses showed:

- No significant deterioration of the lubricant chemical composition,
- No significant water content,
- Improved particle content compared to the new sample indicating excellent filtration.

See Figure 2 for "used" ferrography analysis of the lubricant indicating acceptable operating conditions.

This case is of interest because micropitting has been sporadically seen in similar gear drives operating at pitch line speeds between 73 m/s and 175 m/s. In most cases, micropitting was observed after long years of operation. This gear set was only inspected approximately every four to five years, so it is not certain exactly when the micropitting first occurred.

The gear drives are installed indoors in a heated building. They run at steady loads in continuous operation. The manufacturer reviewed the history of sump temperature and oil analysis for the drives that micropitted. There is no evidence

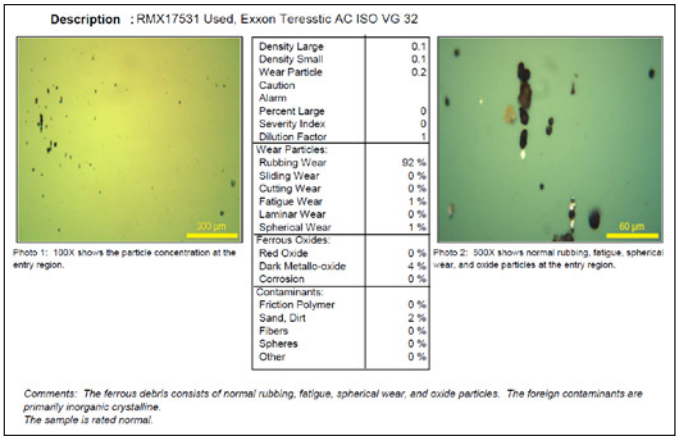

Figure 2—Analytical ferrography of used lubricant. (Photo courtesy of Artec Machine Systems.)

of high temperatures, contaminated lubricant, or nonuniform contact in the gear mesh.

It is interesting to note that Martinaglia's (Ref. 10) testing demonstrates that the zone of highest temperature is located toward the exit end of the tooth face designed with spray ports symmetrically spaced along the spray bars. This result corresponds to the offset pattern in the micropitting seen on this gear set where the tooth flank experienced the highest operating temperatures. We can conclude that the rise in temperature across the face contributed to the onset of micropitting.

In summary, the lubricant and lubrication system for Case 1 performed well throughout the gear set's operation based on the previously mentioned analyses. All data associated with this case's lubricant condition are available upon request.

Calculation Methods for Bulk Temperature and Film Thicknesses

The formulas in ISO/TS 6336-22 were validated with gearing with pitch line velocities between 8 m/s and 60 m/s. Case 1 has a pitch line velocity of 88 m/s. In the previous paper, the Method B calculations arrived at a minimum specific film thickness of 2. While reviewing this example with members of ISO Working Group 6, it was pointed out that the equation for the bulk temperature, θ_M, is not applicable for pitch line velocities above 80 m/s because of significant heat generation from churning and windage that occur at high velocities. Method A is recommended for calculations at pitch line speeds greater than 80 m/s.

A thorough calculation using Method A would model both the contact pressure and bulk temperature across the face of the gear teeth. Unfortunately, *WindowsLDP* does not calculate friction or heat generation within the mesh and creating a model to do so is beyond the time frame for this paper. Instead, we turned to the work of Amendola (Ref. 11) to evaluate the bulk temperature for high-speed gears for scuffing calculations. This work is based on tests conducted by Akazawa (Ref. 12) and Martinaglia (Ref. 10). The result is an equation for bulk temperature that depends on the pitch line velocity for gear sets running at greater than 35 m/s. This equation has been incorporated into AGMA 925-B22 (Ref. 13). Using this equation from AGMA 925, a bulk temperature of 82.93°C resulted and was used in our Method A calculations.

Amendola's previous work (Ref. 14) to correlate MAAG gear predictions to AGMA 925-A03 (Ref. 15) and AGMA 6011-J14 (Ref. 16) uses 100°C for the bulk temperature. To observe the change in the predicted film thickness, 100°C was used for a second set of Method A calculations.

The permissible specific film thickness for Mobil Teresstic AC 32 was calculated using Method B with the geometry of FVA 54 test gears. Unfortunately, no FVA 54 micropitting testing could be found for this lubricant. However, the manufacturer of this gearbox reported that a similar lubricant (Mobil DTE Light, VG 32) used in a similar gearbox was tested and performed to Load Stage 8. Both lubricants have been proven satisfactory in similar applications. Thus, FVA 54 failure Load Stage 8 with 60°C test temperature was used.

Calculation Results

Method A Results

The results using Method A are shown in Table 2.

			θ_M Method	
Name	**Symbol**	**Units**	**Amendola High PLV Calculation**	**MAAG Approx.**
Bulk temperature	θ_M	°C	82.93	100.00
Minimum specific film thickness	λ_{GFmin}	-	1.574	1.149
Permissible specific film thickness	λ_{GFP}	-	0.127	0.127
Safety factor	S_λ	-	12.39	9.04

Table 2—Results using ISO/TS 6336-22, Method A for Case 1.

The pressure distribution and specific film thickness across the contact zone can be seen in Figure 3. The zone of highest pressure and lowest film thickness occurs in the dedendum of the pinion, which corresponds to the location of micropitting. The variation of bulk temperature across the face of the high-speed pinion could not be modeled by *WindowsLDP,* so it does not predict that micropitting will be predominant on the drive end of the face.

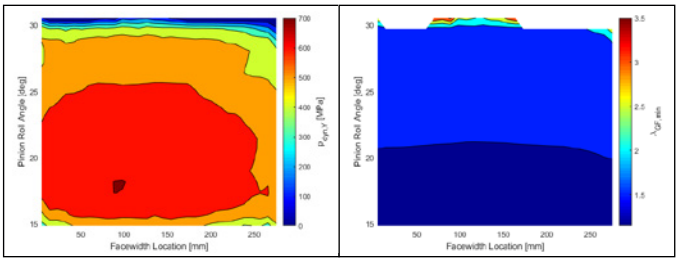

Figure 3—Pressure distribution (left) and specific film thickness (right) across the contact zone for Case 1.

Method B Updated Results

In Table 3, we recalculated the example from the previous paper using Method B for the minimum specific film thickness and bulk temperatures of 82.93°C and 100°C in order to have a closer comparison to the *WindowsLDP* results.

Name	Symbol	Units	θ_M Method		
			ISO/TS 6336-22 Method B (previous paper)	Amendola High PLV Calculation	MAAG Approx.
Bulk temperature	θ_M	°C	60.00	82.93	100.00
Minimum specific film thickness	λ_{GFmin}	-	2.12	1.29	0.95
Permissible specific film thickness	λ_{GFP}	-	0.157	0.127	0.127
Safety factor	S_λ	-	13.48	10.18	7.50

Table 3—Recalculated results using ISO/TS 6336-22, Method B for Case 1.

The Safety Factors

The safety factors that result from all of the calculations—whether using Method A or Method B—are very high. This result occurs when the specific film thickness is much larger than the permissible specific film thickness. However, there are two areas of concern in these calculations:

- The minimum specific film thickness is heavily dependent on the bulk temperature. We did not have a program that can accurately calculate this value. It is also not possible to measure this during the actual operation of the gear drive. We assumed fairly high values for the bulk temperature, but a complete model would contain measured values along the tooth contact, thereby requiring testing with real gears in operating conditions.
- The permissible specific film thickness is based on the assumed performance of Teresstic VG 32 in FVA 54 tests. A more exact value would be derived from standard testing with similar gears. As the permissible value becomes less accurate, the safety factors calculated with ISO/TS 6336-22 are less reliable.
- This gear set operated for billions of stress cycles before surface distress was noted. In such a long life, other applications may be subject to transient torsional, start-up, and shutdown loads that contribute to momentary reductions of film thickness. This gear set was run at even loads without stopping for years. Based on photos of the gear teeth, operational data, and observations, this example appears to have operated under full elastohydrodynamic lubrication (EHL). As such, a lambda greater than one is not a good initial basis for predicting micropitting. Rather, this example suggests that asperity interaction was not a factor in micropitting. Instead, it suggests that micropitting can emerge as a micro-surface Hertzian fatigue phenomenon under full EHL. Only sufficient accumulated stress cycles appear to be needed. Development of a predictive model that incorporates this unique micropitting mechanism is important as gear drive life cycle expectations continue to grow.

Case 2—Wind Turbine Gear Set

Case 2 is a gear set from a 1.5-MW wind turbine at the National Renewable Energy Laboratory (NREL) Flatirons Campus in Colorado. This example is representative of minor micropitting in wind turbine gearing that has operated for five years or more. Micropitting was found in the start of active profile (SAP) of all of the sun pinion teeth. Micropitting and some abrasions were also found higher on the flanks of the sun pinion teeth. The gear set had been installed for just over 8 years. It had produced approximately 6-million kWh of energy in 14,170 hours of grid operation time, representing approximately 8 percent of its minimum design life. Micropitting was noted after just over 6 years of operation, which represents a relatively low number of stress cycles.

Pictures of the micropitting can be seen in Figure 4. The previous paper also contains pictures of the micropitting and details about the gear drive as documented in (Ref. 17). For this paper, all maintenance records were reviewed. In addition, extensive operational data were acquired and analyzed from the turbine's supervisory control and data acquisition (SCADA) system. Reference [18] is publicly available and contains the full documentation for this information.

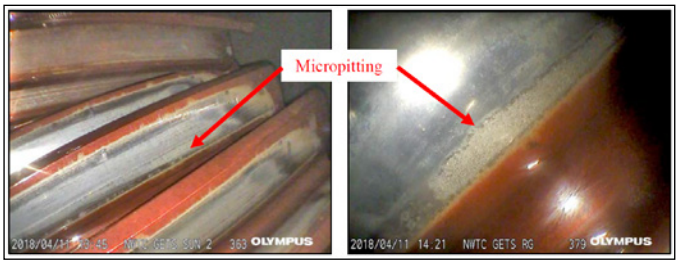

Figure 4—Micropitting on the sun pinion teeth. (Photos by Scott Eatherton, Wind Driven, NREL 61193 and 61194.)

The geometry and lubricant for this case are summarized in Table 4. The gear teeth have adequate profile and lead modifications for the operating loads.

Dimension	Units	Pinion	Gear
Number of teeth	-	27	88
Ratio	-	3.2593	
Center distance	mm	487.51	
Normal module	mm	8.0609	
Face width	mm	200.9	
Outside diameter	mm	247.955	759.079
Pressure angle	degrees	22.5	
Helix angle	degrees	17.584	
Addendum modification coefficient	-	0.0804	0.0804
Surface roughness	µm	0.22	0.55
ISO accuracy grade	-	6	6
Material surface hardness	HRC	59-63	58-62
K_A K_v $K_{H\alpha}$ $K_{H\beta}$ product	-	1.478	
Lubricant	-	Castrol Optigear A320	
Inlet lubricant temperature	°C	50 and 70 (see measured data in Figure 3)	

Table 4—Input data for Case 2.

SCADA Data and Lubricant Analysis

In reviewing the details of the Method B results from the previous paper, questions were raised regarding the gear drive

operating temperature and lubricant condition. This gear drive was well-monitored during its operation. To better understand the influence of its application conditions on the presence of micropitting, three different factors were reviewed:

- *Operating temperatures.* Data were available for the temperature of the oil sump for approximately 7.5 years of the 8 years of operation. Oil sump temperatures ranged from 20°C to 66°C, with the densest cluster being between 40°C and 60°C, as shown in Figure 5 [16]. Later measurements on a replacement gearbox showed the temperature of the outer race of the high-speed-shaft bearing, one of the highest operating temperatures in the gearbox, did not exceed 70°C [19]. Based on this, calculations for the sun pinion were performed with a normal oil temperature of 50°C and a worst-case temperature of 70°C.

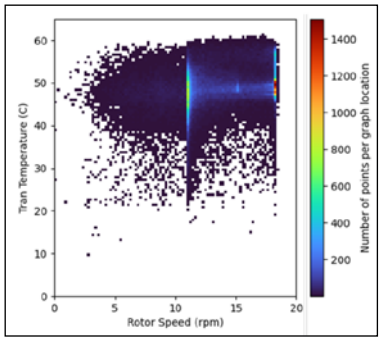

Figure 5—Oil sump temperatures (Ref. 18).

- *Load cases.* Wind turbines operate under varying load conditions. The previous paper applied the mean load condition to calculate the micropitting safety factor. In order to gain an understanding of the running loads that affected the gearing, the operational torque and speed data were mined in both one-second and 10-minute intervals (Ref. 18). The largest amount of time the turbine spent was actually in idle mode, in which the rotor speed is 0–1 rpm and there is no load of the grid operating time, there were high numbers of data points at rotor speeds of 11 rpm (cut-in speed) with loads under 20 percent and 18 rpm (rated speed) at loads ranging from 40 percent to just over 100 percent. An additional collection of points was seen at 13 rpm and relatively light loads under 25 percent. Based on this, it was decided to run calculations at these three load cases summarized in Table 5.

	Units	Original Paper	Cut-In Speed	Intermediate Speed	Rated Speed and Load
Rotor Speed	rpm	18.3	10.91	12.73	18.3
Sun Pinion Speed	rpm	254.17	140.62	164.08	254.17
Sun Pinion Torque	N-m	20,880	3,840	4,080	20,880

Table 5—Load cases for Case 2 calculations.

- *Oil condition.* The NREL report on the gear drive condition [17] mentions that sludge was found in the filter during a late 2017 inspection just prior to removal of the gearbox. In order to determine whether the oil condition influenced the onset of micropitting, especially with respect to water content, the gear drive maintenance records were reviewed. Other than an unexplained brief spike in the water content in 2012, the lubricant condition is normal until the late 2017 inspection. The oil viscosity, particle counts, and water content were otherwise within recommended parameters [18]. From this, it was concluded that the lubricant was well-maintained, resulting in relatively cool, clean, and dry conditions and did not contribute to the micropitting.
- *Castrol Optigear A320 lubricant.* The lubricant supplier was contacted for information related to the lubricant's micropitting resistance. Castrol Optigear A320 has a FVA 54 failure load stage greater than 10 at 60°C and 90°C test temperatures. The permissible specific film thickness of this lubricant was calculated at an oil temperature of 60°C because that provided a more conservative calculation and was representative of the operational data for the wind turbine.

Calculation Results

Method A Results

The results using Method A are shown in Table 6.

At the rated speed and load and an oil temperature of 70°C, the pressure distribution and specific film thickness across the contact zone can be seen in Figure 6. The tooth microgeometry can be seen in the pressure distribution, where low pressure zones are at the root and tip of the pinion tooth. The region of lowest film thickness is located in the dedendum of the pinion between the root clearance and the pitch diameter.

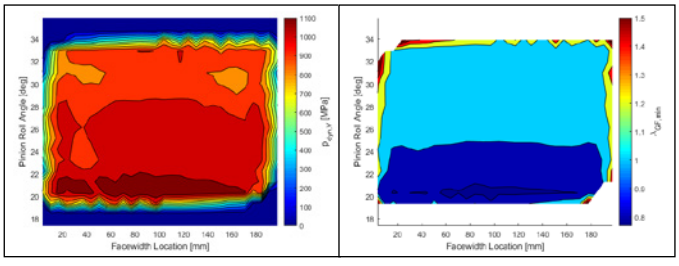

Figure 6—Pressure distribution (left) and specific film thickness (right) across the contact zone for Case 2.

Method B Updated Results

For comparison, Method B calculations were also run using the additional load cases and temperatures. The results are shown in Table 7.

			Load Case					
Name	**Symbol**	**Units**	**Cut-in Speed**		**Intermediate Speed**		**Rated Speed and Load**	
Oil temperature	θ_{oil}	°C	50	70	50	70	50	70
Bulk temperature	θ_M	°C	50.00	70.00	50.00	70.00	50.00	70.00
Minimum specific film thickness	λ_{GFmin}	-	1.742	0.921	1.829	0.964	1.516	0.769
Permissible specific film thickness	λ_{GFP}	-	0.338	0.338	0.338	0.338	0.338	0.338
Safety factor	S_λ	-	5.16	2.73	5.41	2.85	4.48	2.28

Table 6—Results using ISO/TS 6336-22, Method A for Case 2.

			Load Case					
Name	Symbol	Units	Cut-in Speed		Intermediate Speed		Rated Speed and Load	
Oil temperature	θ_{oil}	°C	50	70	50	70	50	70
Bulk temperature	θ_M	°C	50.31	70.32	50.35	70.37	51.70	71.75
Minimum specific film thickness	λ_{GFmin}	-	1.283	0.669	1.412	0.738	1.287	0.695
Permissible specific film thickness	λ_{GFP}	-	0.338	0.338	0.338	0.338	0.338	0.338
Safety factor	S_λ	-	3.80	1.98	4.178	2.18	3.81	2.06

Table 7—Results using ISO/TS 6336-22, Method B for Case 2.

The Safety Factors

The highest load condition for this gear set is at the rated speed. This is also the load case where the lowest safety factors are found. Using Method A, the safety factor is 2.28 with a 70°C oil temperature. However, the gear drive rarely ran with that sump temperature and we would expect the operating safety factor to be closer to 4.48. It is expected that an ISO calculation using Method B will be more conservative than one using Method A. That remains true in this case, with a safety factor of 2.06 when calculated using the 70°C oil temperature.

Guidance in IEC 61400-4

In the last several years, the IEC/ISO joint working group has been revising IEC 61400-4 "Wind turbines - Part 4: Design requires for wind turbine gearboxes" (Ref. 20) to include guidance on the use of ISO/TS 6336-22 for wind turbine gear drives. The calculations in this paper agree with the requirement to use Method A for the calculation of minimum specific film thickness and Method B for the permissible specific film thickness. There is an additional recommendation in IEC 61400-4 to balance the roughness of the pinion and gear teeth for critical gear stages that are not in ISO/TS 6336-22. This gear set does not adhere to that, but neither will many older wind turbine designs.

The draft wind turbine design document also recommends that the safety factor against micropitting should be greater than 2.0 to avoid damage. However, it strongly encourages the engineer to verify the results of the calculation to field experience with similar gear sets and establish a minimum safety factor based on that with values between 1.5 and 2.0. The safety factors calculated for Case 2 approach 2.0 as the oil temperature is raised toward 70°C. However, the gear drive never operated at this temperature. As can be seen in Figure 5, the maximum temperature was 66°C and was between 40°C and 60°C for the majority of the operating time. This is a case where the calculated safety factors should be validated against field experience.

As was noted in "Calculation Results," the gear drive operated at several different load cases based on the wind speed. The load spectra are used to perform a cumulative fatigue damage calculation when wind turbine gearing is evaluated for gear tooth pitting and bending damage. This approach is not possible with micropitting because an S-N curve for micropitting has not yet been established. A calculation in accordance with IEC 61400-4 would be made at the rated speed of the rotor.

Case 3—AGMA Tribology Gear Set

Case 3 is the gearing used in the AGMA Tribology Test Program (Ref. 21). This gearing is similar to FZG "C" gears, but more representative of industrial gears, as they have finer pitch, different tooth counts, and incorporate tip relief and profile modifications to remove interference. They also have axial crowning to increase compressive stress near the center of the face width.

In the previous paper, the micropitting safety factor was calculated with the lubricants that were used in the original tribology test. For this paper, the study performed by Houser (Ref. 22) is referenced. That study was run to test the ISO/TS 6336-22 method by testing with Dexron VI ATF to determine its micropitting load stage. Photos of the micropitted pinion appear in Figure 7.

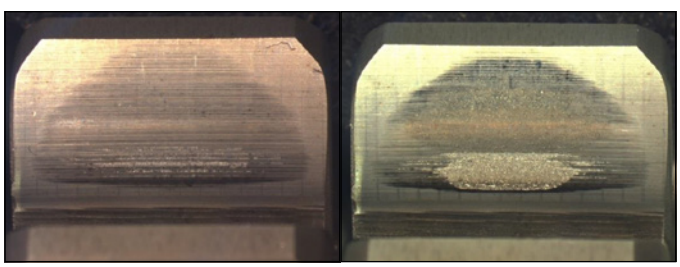

Figure 7—Tooth surfaces of a pinion operated at (left) SKS 9 after 40 hours and (right) SKS 9 after 160 hours. (Photos courtesy of Gearlab at The Ohio State University.)

The calculations with Method B in the last paper resulted in safety factors that were between 1.10 and 1.80, with values decreasing as the load increased. This result is comparable to other calculations of micropitting safety factors that have been reported when micropitting was seen. This paper will compare Method A and Method B calculations with the test results from Houser's study. The calculations were made using the loads for FVA 54 Load Stages 7, 8, 9, and 10 in order to simulate the testing that was performed on the gear set. The geometry and lubricant for this case are summarized in Table 8. The loads appear in Table 9.

Dimension	Units	Pinion	Gear
Number of teeth	-	20	30
Ratio	-	1.50	
Center distance	mm	91.50	
Normal module	mm	3.629	
Face width	mm	13.97	
Outside diameter	mm	82.042	116.716
Pressure angle	degrees	20.00	
Helix angle	degrees	0	
Addendum modification coefficient	-	0.2533	-0.0296
Surface roughness	µm	0.34	0.22
ISO accuracy grade	-	4	5
Material surface hardness	HRC	59-61	59-61
K_A K_v $K_{H\alpha}$ $K_{H\beta}$ product	-	1.0826	
Lubricant	-	Dexron VI ATF	
Inlet lubricant temperature	°C	40 (Measured)	

Table 8—Input data for Case 3.

SKS	Pinion Speed (rpm)	Pinion Torque (N-m)	Nominal Hertzian Contact Stress at Point A (N/mm²)
7	2,250	132.5	1,048
8	2,250	171.6	1,191
9	2,250	215.6	1,333
10	2,250	265.1	1,476

Table 9—Load cases for Case 3 calculations.

Additional Details/Discussions on This Gear Set

The geometry of this example is very close to the FVA 54 test gears and the loads are those used in the load stages for the FVA 54 test. The permissible specific film thickness that is calculated for the lubricant will be representative of the test gearing. It is expected that the safety factors calculated for this case will be predictive of the micropitting found during the testing.

Calculations

Method A Calculation Results

The results using Method A are shown in Table 10.

			SKS Load Stage			
Name	Symbol	Units	7	8	9	10
Bulk temperature	θ_M	°C	53.28	56.58	60.19	64.09
Minimum specific film thickness	λ_{GFmin}	-	0.256	0.224	0.196	0.171
Permissible specific film thickness	λ_{GFP}	-	0.189	0.189	0.189	0.189
Safety factor	S_λ	-	1.35	1.18	1.04	0.90

Table 10—Results using ISO/TS 6336-22, Method A for Case 3.

The pressure distribution and the specific film thickness across the contact zone can be seen for the failure Load Stage 8 loads in Figure 8. The effect of the tooth crowning is clear with the loads centered on the tooth. The influence of the sliding factor on the film thickness is evident in the higher values near the pitch line and lower values near the tooth root.

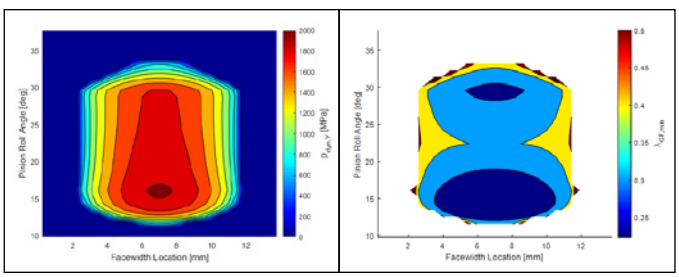

Figure 8—Pressure distribution (left) and specific film thickness (right) across the contact zone for Case 3.

Method B Updated Results

The results of Method B calculations are shown in Table 11.

			SKS Load Stage			
Name	Symbol	Units	7	8	9	10
Bulk temperature	θ_M	°C	53.58	56.91	60.52	64.47
Minimum specific film thickness	λ_{GFmin}	-	0.319	0.273	0.233	0.200
Permissible specific film thickness	λ_{GFP}	-	0.189	0.189	0.189	0.189
Safety factor	S_λ	-	1.69	1.44	1.23	1.06

Table 11—Results using ISO/TS 6336-22, Method B for Case 3.

The Safety Factors

Using both Method A and Method B, the calculated safety factors are well-aligned to the micropitting seen on the test gears. Significant micropitting was seen between Load Stages 8 and 9 with low values of safety factors at these stages.

Conclusions

The details of the calculations of these case studies are quite lengthy. The drawings and details of the profile and lead modifications are also proprietary. As a result, the authors can provide specific details upon request.

This investigation has reviewed calculations using ISO/TS 6336-22 Method A and Method B, comparing the results against field results. In the process of writing both papers, extensive reviews have been made of geometry, surface roughness, load conditions, and lubricant conditions. These reviews were done to best understand the influences of micropitting on each example and the applicability of the calculations to the results. The following conclusions about the methods can be made.

- *The safety factors calculated using Method A and Method B did not predict micropitting for Cases 1 and 2.* Both cases have high safety factors, but experienced micropitting in application.
- *Permissible specific film thickness.* The permissible specific film thickness is a significant factor in the calculation of a micropitting safety factor. It is important to use a value that is representative of the gear set being evaluated.
  - This value is best when measured from testing of real gear sets in application conditions until they micropit. This is not always practical or possible.
  - If testing with real gears is not possible, a calculation using the results of FVA 54 testing can be used. However, FVA 54 testing is a test of the micropitting resistance of a lubricant using gearing that is designed to micropit. The resulting permissible film thickness will have a degree of uncertainty based on how different the gearing and operating conditions are from the FVA 54 test.
- *Fatigue limits for micropitting.* Case 1 ran at steady load and speed for much longer than what would be the endurance limit for the classic bending or pitting failures. In addition, the condition of the nondamaged flank areas indicates that the gearing operated in a full EHL regime throughout its life. The *WindowsLDP* analysis shows that the entire face of each tooth carried the contact. Despite these good operating conditions, the teeth experienced micropitting after billions of cycles. This outcome leads one to question whether micropitting is solely predicted by film thickness, or whether additional fatigue considerations play a role.
- *Minimum specific film thickness.* Method B is a general calculation model for the minimum specific film thickness. The engineer is advised that a more thorough analysis uses Method A. However, the engineer is left to decide how to determine the pressures and temperatures within the contact zone when using Method A.
- *Influence of surface roughness method.* ISO/TS 6336-22 uses the arithmetic mean roughness value (Ra) to assess the influence of the surface finish on the specific film thicknesses. Recent tribological work has utilized the root-mean-square roughness (Rq) or maximum height of profile (Rz). In order to test whether the use of these parameters would change the results of the calculations, measured values of Rz from the gearing in Case 2 were used to calculate the specific film thickness. Measured values of FVA 54 test gearing were used to calculate the permissible specific film thickness. Specific film thickness decreased when using Rz. The resulting safety factor also decreased, but it is hard to say whether it is more predictive of micropitting. More review is needed on this topic.

			Roughness Method	
Name	**Symbol**	**Units**	**Ra**	**Rz**
Effective roughness[1]	Ra, Rz	μm	0.385	4.315
Minimum specific film thickness	λ_{GFmin}	-	0.653	0.058
Permissible specific film thickness	λ_{GFP}	-	0.338	0.048
Safety factor	S_λ	-	1.932	1.212

[1] Effective roughness using Ra is the arithmetic mean value. Effective roughness using Rz is the root-mean-square value.

Table 12—Results of using alternate roughness parameters, Case 2, Method B.

In general, the methods in ISO/TS 6336-22 work best when the engineer has complete knowledge of the design, manufacturing, operating conditions, and service life of the gear set and its lubricant. Pinnekamp (Ref. 23) noted that confidence in the safety factor against micropitting relies on the engineer's knowledge of the operating conditions and the quality of their calculations. The safety factor must be compared to the results of the tests with similar gears when there is low confidence in the methods.

Future Work

As the science behind predicting micropitting continues to evolve, some future work is needed for ISO/TS 6336-22. Future development should arrive at safety factors that do not require comparison to similar gearing for interpretation. Additional recommendations are to:

- Continue to develop a method to establish the permissible specific film thickness of the lubricant when testing of real gears is not possible. If results from FVA 54 lubricant tests must be used, it would be helpful to have a method to scale the data to the application geometry and loads.
- Improve the guidance to lead the engineer in the complete use of Method A, including all factors for consideration (e.g., load, temperature, surface topography, etc.).
- Develop a test procedure to evaluate the S-N relationship for micropitting so the impact of accumulated stress cycles can be established when evaluating for the risk of micropitting. Further, developing a predictive model that incorporates this unique micropitting mechanism is important as gear drive life cycle expectations continue to grow.

Acknowledgments

Many thanks to the contributors to this paper:

- *WindowsLDP* data was provided by The Ohio State University.
- Artec Machine Systems provided the geometry and application data for the compressor gear set in Case 1.
- NREL and General Electric Renewables provided geometry and application data for the wind turbine gear set in Case 2.
- REM Surface Engineering provided the surface roughness analyses for all three cases.
- Regal Rexnord provided all support for the Method B calculations and analysis.

This work was authored in part by the National Renewable Energy Laboratory, operated by Alliance for Sustainable

Energy, LLC, for the US Department of Energy (DOE) under Contract No. DE-AC36-08GO28308. Funding was provided by the US Department of Energy Office of Energy Efficiency and Renewable Energy Wind Energy Technologies Office. The views expressed in the article do not necessarily represent the views of the DOE or the US Government. The US Government retains and the publisher, by accepting the article for publication, acknowledges that the US Government retains a nonexclusive, paid-up, irrevocable, worldwide license to publish or reproduce the published form of this work, or allow others to do so, for US Government purposes.

References

1. ISO/TC 60/SC 2/WG 6, 2018, "Calculation of load capacity of spur and helical gears—Part 22: Calculation of micropitting load capacity," ISO/TS 6336-22.
2. R. Olson, M. Michaud, J. Keller, 2020, "Case Study of ISO/TS 6336-22 Micropitting Calculation," AGMA Fall Technical Meeting, Paper 20FTM07.
3. FVA Information Sheet No. 54/I-IV, "Test procedure for the investigation of the micro-pitting capacity of gear lubricants," July 1993.
4. *WindowsLDP* (Load Distribution Program), Gear and Power Transmission Research Laboratory, The Ohio State University, Columbus, Ohio, 2021.
5. Singh, A., Houser, D. R., "Analysis of off-line of action contact at the tips of gear teeth," SAE Technical Paper, No. 941761, 1994.
6. Yau, E., Busby, H. R., Houser, D. R., "A Rayleigh-Ritz approach to modeling bending and shear deflections of gear teeth," *Computers & Structures,* Vol. 50, No. 5, 705–713, 1994.
7. Stegemiller, M. E., Houser, D. R., "A three-dimensional analysis of the base flexibility of gear teeth," *Journal of Mechanical Design,* Vol. 115, 186–192, 1993.
8. Weber, C., "The deformations of loaded gears and the effect on their load-carrying capacity," Sponsored research (Germany), British Dept. of Scientific and Industrial Research, Report No. 3, 1949.
9. Conry, T. F., Seireg, A., "A mathematical programming technique for the evaluation of load distribution and optimal modifications for gear systems," *Journal of Manufacturing Science and Engineering,* Vol. 95, 1115–1122, 1973.
10. Martinaglia, L., "Thermal Behavior of High-Speed Gears and Tooth Corrections for Such Gears"; ASME/AGMA International Symposium on Gearing and Transmissions, 1972.
11. Amendola, J., Amendola, J. III, Errichello, R., "Defining the Tooth Flank Temperature in High Speed Gears", AGMA Fall Technical Meeting, Paper 21FTM08.
12. Akazawa, M., Tejima, T., Narita, T., "Full Scale Test of High Speed, High Powered Gear Unit – Helical Gears of 25,000 PSI at 200 m/s PLV": ASME Paper No. 80-C2/DET-4, 1980.
13. "Effect of Lubrication on Gear Surface Distress," AGMA 925-B22.
14. Amendola, J., Amendola, J. III, Errichello, R., "Calculated Scuffing Risk: Correlating AGMA 925-A03, AGMA 6011-J14, and Original MAAG Gear Predictions," AGMA Fall Technical Meeting, Paper 19FTM24.
15. "Effect of Lubrication on Gear Surface Distress," AGMA 925-A03.
16. "Specification for High Speed Helical Gear Units," AGMA 6011-J14.
17. Keller, J., Michaud, M., and Lambert, S., 2020, "Report of the Condition of a General Electric Transportation Systems Gearbox" (Technical Report). Golden, CO: National Renewable Energy Laboratory. NREL/TP-5000-76004, *https://www.nrel.gov/docs/fy20osti/76004.pdf*
18. Keller, J. et al. 2022. "Insights on Wind Turbine Maintenance from the Usage History of a General Electric Transportation Systems Gearbox" (Technical Report). Golden, CO: National Renewable Energy Laboratory. NREL/TP-5000-82704. *http://www.nrel.gov/docs/fy22osti/82704.pdf*
19. Keller, Jonathan, Yi Guo, and Latha Sethuraman. 2019. "Uptower Investigation of Main and High-Speed-Shaft Bearing Reliability" (Technical Report). Golden, CO: National Renewable Energy Laboratory. NREL/TP-5000-71529. *https://www.nrel.gov/docs/fy19osti/71529.pdf*
20. IEC/TC 88 and ISO/TC 60, "Wind turbines—Part 4: Design requirements for wind turbine gearboxes," IEC 61400-4:2012, International Electrotechnical Commission.
21. Bradley, W.A., "AGMA Tribology Test Report," AGMA Foundation Report, 2008.
22. Houser, D.R. and Shon S., 2015, "An Experimental Evaluation of the Procedures of the ISO/TR 15144 Technical Report for the Prediction of Micropitting," AGMA Fall Technical Meeting, Paper 15FTM25.
23. Pinnekamp, B. and Heider, M., 2015, "Calculating the Risk of Micropitting Using ISO Technical Report 15144-1:2014—Validation with Practical Applications," AGMA Fall Technical Meeting, Paper 15FTM26.

Robin Olson is the director of application engineering in the Engineered Gear group of Regal Rexnord's Motion Control Solutions division. She started her career in gear engineering with the Falk Corporation in 1995 and has held previous roles in engineering software and analysis, sustaining engineering, warranty, test lab, and technical services. She has bachelor's and master's degrees, both in Physics. She has participated in various AGMA Technical Committees since 1995 and is currently a member of the Helical Gear Rating Committee. She has the honor of representing the United States on Working Group 6 of ISO TC 60, covering the topic of Gears.

David Talbot is an assistant professor at The Ohio State University Department of Mechanical and Aerospace Engineering. His research focuses on multi-disciplinary power transmission problems within the aerospace, transportation, wind energy, and industrial gearbox industries. His specific research investigations include load distribution modeling of power transmission components, gear, bearing, and power transmission system efficiency modeling and measurement, gear dynamics and vibrations, and gear manufacturing process simulation.

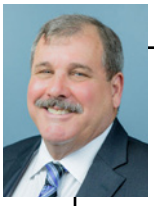

Mark Michaud recently celebrated his 40th year with REM Surface Engineering. Mark is the inventor and pioneer of REM's chemically accelerated finishing technology; currently serving as technical fellow. Mark Michaud is a leading scientist and technical mentor and continues to play a crucial role in the company's future. Mark has authored numerous patents and technical papers and served a term on the AGMA board of directors. Mark continues to serve as vice-chair of the AGMA Aerospace Committee, as a member of the AGMA Wind Turbine Committee, and as a shadow delegate to ISO 614-4 Wind Turbine Committee. He graduated with a bachelor's degree in chemistry from Reed College and an MBA from the University of Hartford.

Jon Keller is the team leader for wind turbine drivetrain technology at NREL. Jon leads projects ranging from the development and verification of new drivetrains with improved performance, power density, and efficiency and to in-depth research investigations of failure modes and improvement in reliability of existing drivetrains often conducted in the dynamometers or field turbines. Prior to joining NREL, Jon worked for the US Army at Redstone Arsenal, AL, for 10 years, where he developed condition monitoring systems for Army rotorcraft to reduce the cost and maintenance burdens while increasing availability and safety. His Ph.D. is in aerospace engineering from Penn State University.

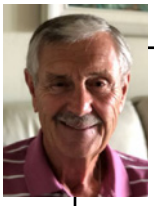

John Amendola, Sr. is an executive officer and chairman of the board of Artec Machine Systems where he has been working for 50 years. Prior employment was with Western Gear, Texaco & Boeing Co. where he operated a full load four square locked torque test stand for helicopter gears. He is currently an active member of AGMA Helical Gear Rating & Lubrication Committees, active chairman of AGMA Enclosed High Speed Units Committee, a member of the US TAG to ISO TC60, and a member of the American Petroleum Institute 613-6 Standards Task Force. John holds a Bachelor of Mechanical Engineering degree from Villanova University and a Master of Science degree in Mechanical Engineering from (NYU) Brooklyn Polytechnic Institute. Amendola is a recipient of the AGMA TDEC Award.